Hindawi
Geofluids
Volume 2022, Article ID 4697730, 17 pages
https://doi.org/10.1155/2022/4697730

Research Article

Design and Analysis of Grouting Pressure in Slurry Pipe Jacking Based on the Surrounding Soil Stability Mechanical Characteristics

Jimin Liu[1,2] **Hua Cheng**[1,2,3] **Haibing Cai**[1,2] **and Xuesong Wang**[1,2]

[1]School of Civil Engineering and Architecture, Anhui University of Science and Technology, Huainan 232001, China
[2]State Key Laboratory of Mining Response and Disaster Prevention and Control in Deep Coal Mine, Anhui University of Science and Technology, China
[3]School of Resources and Environmental Engineering, Anhui University, Hefei 230601, China

Correspondence should be addressed to Hua Cheng; hcheng@aust.edu.cn

Received 26 April 2022; Accepted 31 May 2022; Published 16 June 2022

Academic Editor: Di Feng

In slurry pipe jacking, lubricant slurry is commonly used to sustain against the displacement and pressure of the overcut area and reduce the interface friction of pipelines. Therefore, a reasonable grouting pressure should ensure the stability of surrounding soils, which is raised as a new method in this study. Not only ensure the grouting pressure is not too small to support the stratum effectively and reduce the frictional resistance but also ensure that the grouting pressure will not be too large to produce excessive deformation and affect the surrounding environment. First of all, the influence of grouting pressure on the stability of surrounding soil is analyzed, and the mechanical model of slurry grouting expansion is established. Then, the minimum grouting pressure is designed from the critical balance between radial expansion tension by grouting and loose earth pressure by jacking excavation, and the maximum grouting pressure is designed from the critical expansion pressure caused by grouting splitting. Finally, the rationality of grouting pressure design is proved by the engineering example of a slurry pipe-jacking project near Haikou Meilan Airport and on-site GPR detection test. All these work aims to raise a new theoretical solution of grouting pressure and provide theoretical reference for similar projects.

1. Introduction

Slurry pipe jacking is a special construction jacking method with perfect friction resistance reduction effect, which is widely used in water supply, sewage, coal mines, communication, and electricity pipelines all over the world [1–4]. In the construction of slurry pipe jacking, the grouting pressure is the controlling parameter, which is focused by academics and engineerings. At present, the grouting pressure is mostly determined by empirical method recommended in standard or specification at home and abroad, which adopts the method of increasing 20~50 kPa on the basis of water pressure [5, 6]. This empirical method has great randomness, and the theoretical research of grouting pressure is far from the actual needs of projects, so a further discussion is demanded.

In pipe jacking engineering, bentonite or polymer slurries are commonly injected into the surrounding soil from precast ports on the surface of pipelines and the shield tail space. Field studies have shown that bentonite and plasticizers can reduce the friction by about 20–25%, and combining plasticizers with bentonite or polymers can reduce the friction by about 65–75% in soft soils [7, 8]. Furthermore, Tang et al. studied the construction of pipe jacking in deep-buried coal mine strata and found a higher grouting pressure is required to balance high ground pressure. And the leakage of bentonite grout caused bad support for surrounding rocks and poor lubrication effect [9–11]. Niu et al., Wang et al., Ren et al., and Ke and Lai studied the ground deformation and the lateral disturbance range due to grouting and found that the surface settlement was, respectively, reduced by 30% and 10.8% when the grouting pressure was increased from 100 kPa to 300 kPa [12–15]. All these studies revealed that the grouting pressure greatly influence the results of frictional resistance reduction and the surrounding environment. Therefore, a reasonable grouting pressure should be designed to ensure the frictional resistance reduction effect and protect the surrounding environment as well.

To achieve these two design objectives, the mechanics of friction resistance reduction by grouting and the disturbance mechanism to surrounding soil should be analyzed firstly. Many scholars have done a lot of valuable researches on this, which provided great inspiration and help in solving this problem. Wei et al. pointed out that the slurry infiltrates into the pores of the soil layer under pressure to form a slurry-soil mixture, which is commonly known as mud sleeve and plays a key role in pipeline lubrication and frictional resistance reduction. The grouting of slurry pipe jacking is just like filter paper under pressure to support the surrounding soil and reduce frictional resistance around the pipelines [16]. Shimada et al., Namli et al., Staheli, and Cheng further pointed out that the effective support to surrounding soils is the premise of lubrication and frictional resistance reduction and the grouting pressure decide the supporting effect to surrounding soils greatly [17–20]. Long et al., Wang et al., Wang and Long, and Yang et al. also agreed with the above views and proposed that the slurry should have complete performance of sustain protection and lubrication resistance [21–24]. Based on this, they designed slurry mix proportion of clay-free slurry for long-distance pipe jacking and Kaolin polymer slurry for large-diameter pipe jacking in desert areas. It can be seen that the radial slurry expansion tension on soil directly affects the stability of surrounding soil near the mud sleeve. When the soil is stable, the slurry acts on the segment smoothly and effectively reduces the friction resistance. Therefore, the minimum grouting pressure can be designed from the critical stable condition.

Besides, Yuan et al. analyzed the disturbed soil in the pile-soil interaction system [25–28]. Ye et al. pointed out that synchronous grouting produces radial pressure on the surrounding soil, forcing the surrounding soil to deform greatly. When the grouting pressure is high enough, the slurry will split the surrounding soil, causing excessive deformation and surface uplift, or the segments will float and crack locally or as a whole [29, 30]. Furtherly, Zou et al. studied the mechanical mechanism of soil splitting grouting and the splitting grouting pressure based on hydraulic fracturing theory systematically [31, 32]. All these studies revealed that there occurs the critical spitting pressure which greatly affected the surrounding environment. Only when the surrounding soil near mud sleeve is stable, the surrounding environment is not affected, and the maximum grouting pressure can be designed from the critical splitting pressure caused by grouting disturbance.

Therefore, the design value of grouting pressure can be analyzed from the mechanical mechanism of the surrounding soil and designed according to the necessary conditions for maintaining the stability of surrounding soils. The minimum grouting pressure is designed in the critical state of surrounding soil stability which retains the static equilibrium between radial expansion tension caused by grouting and the radial loose earth pressure caused by jacking excavation, and the maximum grouting pressure is also designed from the critical state of surrounding soil stability which arises slurry grouting splitting. The design thinking map is shown in Figure 1. Furthermore, as the soil around pipelines is radially expanded and the stress field is redistributed due to the effect of grouting pressure, synchronous grouting in slurry pipe jacking can be regarded as the cylindrical hole expansion under expansion pressure. And its mechanical model of radial expansion and the theoretical solution due to grouting can be analyzed by cavity expansion methods, which is an effective stress field calculation method in geomechanics especially good at solving the stress problem controlled by pressure such as tunnel excavation, bolt support, shaft sinking, and in situ tests such as static CPT [33–36].

2. Influence Analysis of Grouting Pressure

In pipe jacking engineering, the external diameter caused by TBM excavating will be greater than the external diameter of pipelines, generally about 20-50 mm, which is the so-called overcut area. When synchronous grouting happens, the slurry will be injected into the overcut area to compact the soil, break the original stress balance, and change the distribution of stress and deformation. With the injection of slurry and the action of grouting pressure, the bentonite slurry, underground pipelines, and surrounding soil begin to interact with each other, the stress-strain distribution caused by grouting becomes complex. Figure 2 shows the whole process of grouting disturbance in slurry pipe jacking. Referred R_e as the excavation radius of micro tunnel boring machine, R_p as the outer radius of segment, and the difference between them is ΔR. δ is the thickness of filter cake.

At the beginning of grouting, the slurry is injected through the precast grouting hole on the segment and fills the gap in the overcut area in time. And a cylindrical shell grouting layer is formed around pipelines, which is shown in Figure 2(a).

With the injection of lubricating slurry, the slurry will interact with the soil. Under the action of grouting pressure, the slurry gradually infiltrates and diffuses into the stratum and forms the slurry-soil mixture. First, the water between the soil particles is squeezed and diffused, and then the slurry penetrates into the pores between the soil particles. When the slurry reaches the possible penetration depth, it will stay still and formed many dense infiltration blocks due to the thixotropy of the slurry, as shown in Figure 2(b).

Under the continuous extrusion of grouting pressure, the infiltration blocks increase gradually. When the infiltration blocks are bonded and consolidated, a relatively dense and impermeable mud sleeve will form, which is called filter cake. The filter cake layer prevents the slurry from continuing to penetrate into the stratum and begins to radially support the surrounding soil. It acts together with the loose

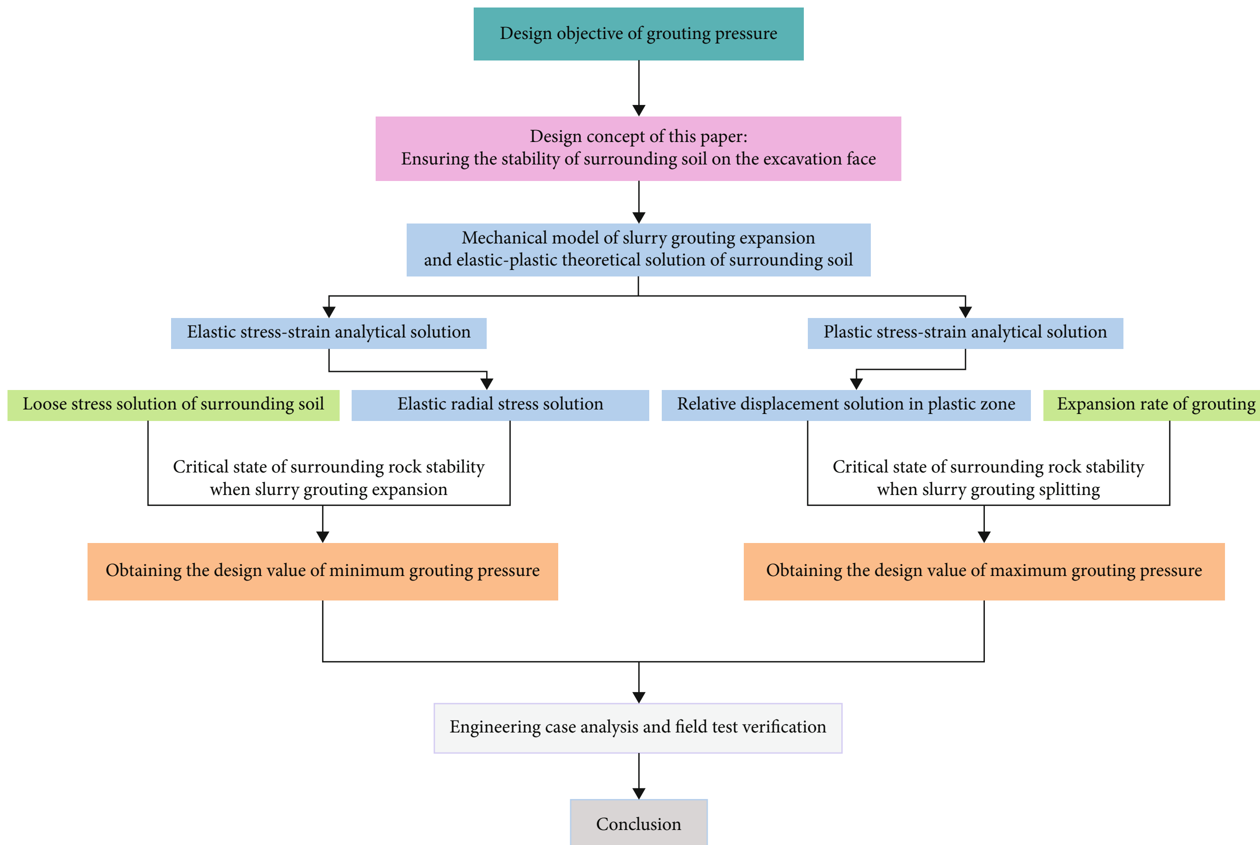

FIGURE 1: Design idea map of slurry grouting pressure.

stress caused by excavation and affects the stability of the surrounding soil near the excavation hole, as shown in Figure 2(c).

If the grouting pressure is taken at a reasonable value, the radial expansion stress σ_δ is greater than the loose radial stress σ_n, and the slurry-soil mixture is not split by grouting, the filter cake will effectively support the surrounding soil, which will cause the surrounding soil near the excavation hole to be in a stable state. As the excavation hole under the action of grouting pressure is stable, the slurry can be injected continuously and contact with the outer surface of pipelines in direct, which leads to a significant frictional resistance reduction and effective lubrication effect, as shown in Figure 2(d).

On the contrary, if the grouting pressure value is taken too small, the radial expansion stress at the slurry-soil interface is less than the loose radial stress, the filter cake will not be able to effectively support the soil, and the surrounding soil near the filter cake will lose its stability, and collapse on pipelines which would increase the frictional resistance and reduce the lubricating effect evidently, as shown in Figure 2(e). In the meanwhile, if the grouting pressure value is taken too large, the slurry-soil mixture will be split by grouting, large deformation will appear in stratum, and the surrounding soil near the excavation hole will also lose its stability, causing surface uplift furtherly and affect the surrounding environment.

From the above analysis, it can be seen that

(1) The slurry forms a cylindrical shell grouting layer in overcut area during synchronous grouting in pipe jacking. The slurry grouting compresses the soil along the radial direction of pipelines, dissipates the pore water in the original stratum, destroys its internal structure and directly affects the stress and displacement of the surrounding soil, and forms the secondary distribution after grouting disturbance. The surrounding soil disturbed by synchronous grouting can be regarded as slurry grouting expansion

(2) Grouting pressure has a great influence on the stability of surrounding soil near the excavation face. Only when the surrounding soil on the excavation hole remains stable under the action of grouting pressure can the effect of reduced resistance grouting and the surrounding environment be ensured. The minimum grouting pressure ensures the stability of surrounding soil when there is good resistance reduction effect, and the maximum grouting pressure ensures the stability of surrounding soil when the slurry splits the stratum and destroys the surrounding environment

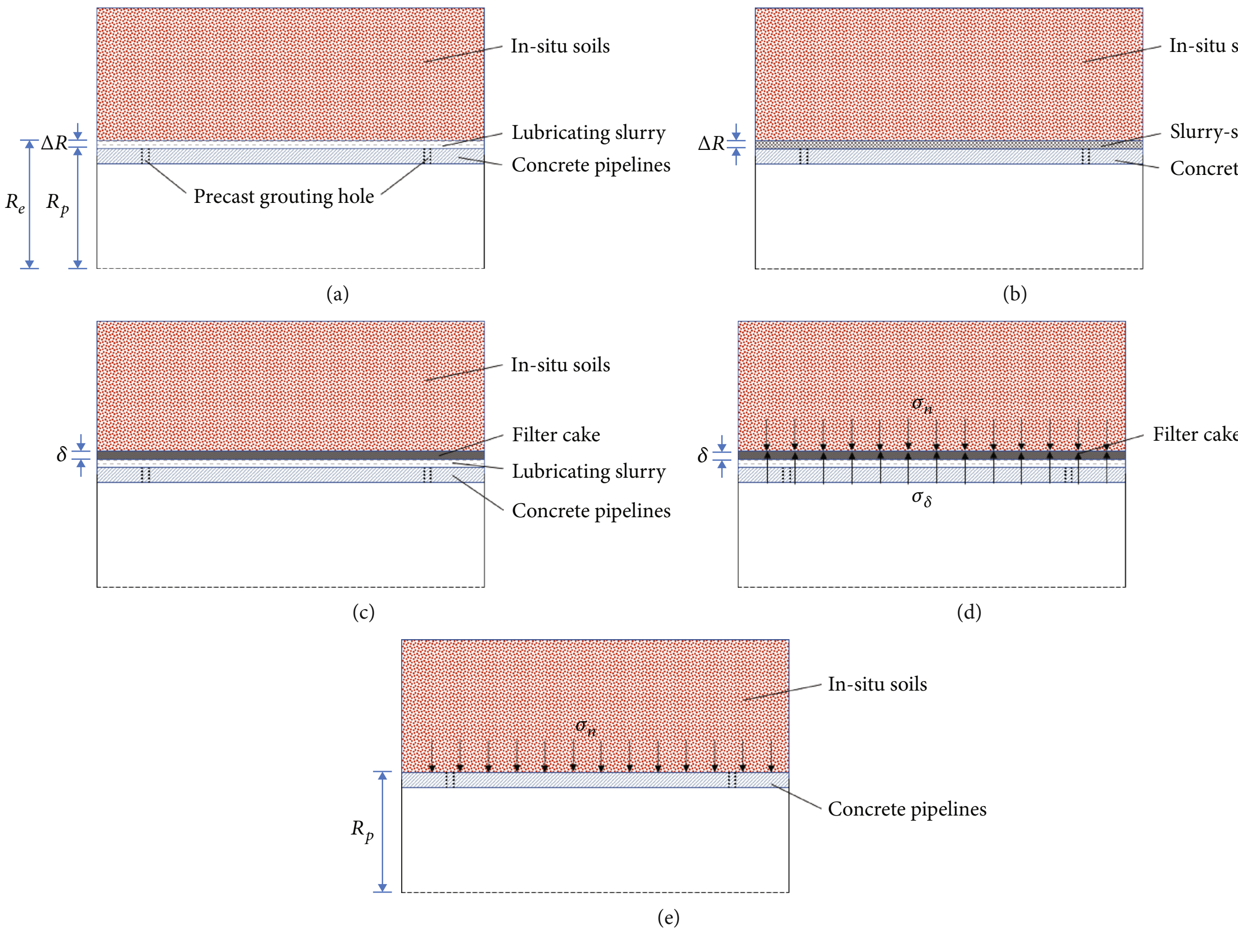

Figure 2: Schematic diagram of the whole process of grouting disturbance. (a) Initial grouting and filling overcut area. (b) Slurry seepage and forming slurry-soil mixture. (c) The slurry compresses the soil and forms a filter cake. (d) The surrounding soil maintains it stability at excavation hole. (e) The surrounding soil lose it stability at excavation hole.

3. Theoretical Design of Grouting Pressure

3.1. Slurry Grouting Expansion Mechanical Model and Theoretical Analysis Solution. Assuming that the slurry fully fills the overcut area, uniformly squeezes, and compacts the surrounding soil, the slurry expansion during synchronous grouting in pipe jacking can be simplified as the expansion of cylindrical hole with axisymmetric plane strain in the infinite half-space under the action of uniform internal pressure. Therefore, according to the cylindrical cavity expansion method, the mechanical model can be established, and the following basic assumptions can be made

(1) The surrounding soil is continuous homogeneous elastic-plastic medium, and the isotropy of initial stress is considered. When the soil is plastic failure, it obeys the uniform strength criterion. This is because the unified strength criterion fully considers the effect of medium principal stress, and the theory has a unified mechanical model and unified mathematical modeling equation and expression. It can be applied to various materials and is conductive to engineering popularization. The unified strength criterion under plane strain conditions can be expressed as

$$\sigma_r = M\sigma_\varphi + \sigma_0, \tag{1}$$

$$M = \frac{2(1+b)(1+\sin\varphi) + mb(\sin\varphi - 1)}{[2(1+b) - mb](1-\sin\varphi)}, \tag{2}$$

$$\sigma_0 = \frac{4(1+b)c\cos\varphi}{[2(1+b) - mb](1-\sin\varphi)}, \tag{3}$$

where m is the ratio of the medium principal stress to the average of the large and small principal stresses. In the plane strain condition, usually take $m = 1$, b is the parameter characterizing the influence degree of principal stress in the unified strength theory. When $b = 1/2$, the soil is in plasticity and a new criterion between Mohr-Coulomb strength theory, and Yu's double shear strength theory can be obtained, which has a good simulation effect.

(2) Regardless of the pipeline deflection during jacking, it is considered that the reaming pressure is perpendicular to the longitudinal axis and is symmetrically and evenly stressed along the jacking direction. The stress of surrounding soil after slurry grouting expansion can be treated as the condition of plane strain

When the reaming pressure is small, the surrounding soil only undergoes elastic deformation, as shown in Figure 3(a). Referred a_0 as the initial radius, the hole radius after expansion is called the expanding radius a. Referred p_0 as the initial pressure of the hole, and p is called the expansion pressure of the hole. When the uniformly distributed internal pressure changes from p_0 to p, the radius of the hole changes from a_0 to a. During synchronous grouting in pipe jacking, the initial hole radius a_0 is taken as the outer radius of pipelines R_p, which means $a_0 = R_p$. The initial pressure of the hole p_0 is the original stress at infinity, which is generally considered as $p_0 = \gamma z$, where γ is the gravity of soil and z is the depth of pipeline center from the ground surface. Considering the influence of hydrostatic pressure during expansion, the reaming pressure p is taken as the difference between the grouting pressure p_s and the hydrostatic pressure p_w, which means $p = p_s - p_w$. With the continuous increase of internal pressure, the soil around the hole begins to yield, from the original overall elastic state to the state of containing both elastic and plastic regions. In the range of $a < r < r_p$, it forms circular plastic zone. In the range of $r \geq r_p$, it forms the plastic zone, which is shown in Figure 3. Here, the radius of the plastic zone is r_p, and the corresponding radial stress is the critical plastic pressure p_y.

(3) The soil in the elastic zone obeys the linear elastic hypothesis of small deformation, and their deformation satisfies the geometric and physical equations, which can be expresses as

$$\begin{cases} \varepsilon_r = -\dfrac{du_r}{d_r}, \\ \varepsilon_\theta = -\dfrac{u_r}{r}, \end{cases} \tag{4}$$

$$\begin{cases} \varepsilon_r = \dfrac{1-\nu^2}{E}\left(\sigma_r - \dfrac{\nu}{1-\nu}\sigma_\theta\right), \\ \varepsilon_\theta = \dfrac{1-\nu^2}{E}\left(\sigma_\theta - \dfrac{\nu}{1-\nu}\sigma_r\right), \end{cases} \tag{5}$$

where ε_r and ε_θ are radial and tangential strain, respectively, E is elastic modulus, and ν is Poisson's ratio.

The yield soil in the plastic zone satisfies the flow rule associated with the unified strength criterion

$$d_{\varepsilon_{ij}^p} = d_\lambda \frac{\partial F}{\partial \sigma_{ij}}. \tag{6}$$

In the meanwhile, the soils in the elastic-plastic zone all satisfy the coordination equation of soil deformation

$$\frac{d_{\varepsilon_\varphi}}{d_r} + \frac{\varepsilon_\varphi - \varepsilon_r}{r} = 0. \tag{7}$$

Based on the above three basic assumptions, the analytical solutions of elastic and plastic stresses, strains, and displacements of the surrounding soil in slurry grouting expansion can be established. From the basic assumption 2, when the expansion pressure is low and satisfies $p < p_y$, the soil around the hole is in an elastic state, as shown in Figure 3(a). The soils around the cylindrical hole satisfy the differential equation of stress balance

$$r\frac{\partial \sigma_r}{\partial r} + (\sigma_r - \sigma_\theta) = 0, \tag{8}$$

where σ_r and σ_θ are radial and tangential normal stress, respectively, and r is polar radius.

At $r = a$, the radial stress of soil takes as p, at infinity, the radial stress of soil takes as p_0. So the boundary condition can be expressed as

$$\begin{cases} \sigma_r|_{r=a} = p, \\ \sigma_r|_{r\longrightarrow\infty} = p_0. \end{cases} \tag{9}$$

From the basic assumption 3 and combining equations (4), (5), (8), and (9), the stress, strain, and displacement in elastic zone are obtained as the following

$$\begin{cases} \sigma_r = p_0 + (p - p_0)\left(\dfrac{a}{r}\right)^2, \\ \sigma_\varphi = p_0 - (p - p_0)\left(\dfrac{a}{r}\right)^2, \end{cases} \tag{10}$$

$$\begin{cases} \varepsilon_r = \dfrac{1}{2G}(p - p_0)\left(\dfrac{a}{r}\right)^2, \\ \varepsilon_\varphi = -\dfrac{1}{2G}(p - p_0)\left(\dfrac{a}{r}\right)^2, \end{cases} \tag{11}$$

$$u_r = \frac{p - p_0}{2G}\left(\frac{a}{r}\right)^2 r, \tag{12}$$

where G is the shear modulus of soil and satisfies $G = E/2(1 + \nu)$.

When the expansion pressure increases and satisfies $p > p_y$, from the basic assumption 2, the deformation in the region of $r > r_p$ is also in elastic state. So its solutions of stress, strain, and displacement in the area satisfy the above equations (10), (11), and (12) and can be expressed as

$$\begin{cases} \sigma_r = p_0 + \left(p_y - p_0\right)\left(\dfrac{r_p}{r}\right)^2, \\ \sigma_\varphi = p_0 - \left(p_y - p_0\right)\left(\dfrac{r_p}{r}\right)^2, \end{cases} \tag{13}$$

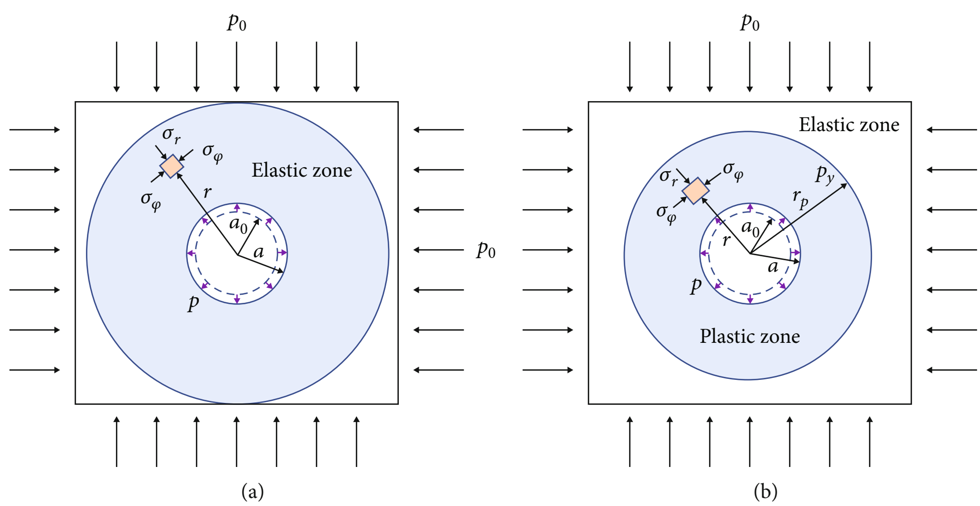

FIGURE 3: Mechanical model of radial expansion of slurry reaming. (a) Elastic stress in the whole region. (b) Elastic and plastic stress in the whole region.

$$\begin{cases} \varepsilon_r = \dfrac{1}{2G}\left(p_y - p_0\right)\left(r_p\right)^2, \\ \varepsilon_\varphi = -\dfrac{1}{2G}\left(p_y - p_0\right)\left(\dfrac{r_p}{r}\right)^2, \end{cases} \tag{14}$$

$$u_r = \frac{p_y - p_0}{2G}\left(\frac{r_p}{r}\right)^2 r. \tag{15}$$

Substituting equation (13) into the unified strength criterion (1), we get the critical plastic pressure

$$p_y = \frac{2Mp_0 + \sigma_0}{1 + M}. \tag{16}$$

As the soil in the plastic region satisfies both the yield criterion and the differential equation of stress balance. Combining equations (1), (2), (3), and (8), the stress in plastic zone should satisfy the following.

$$\frac{d\sigma_r}{d_r} + \left(1 - \frac{1}{M}\right)\frac{\sigma_r}{r} + \frac{1}{M}\frac{\sigma_0}{r} = 0. \tag{17}$$

Solving this differential equation, we get

$$\sigma_r = K\left(\frac{1}{r}\right)^{(1-1/M)} - \frac{\sigma_0}{M-1}, \tag{18}$$

where K is the integration constant.

This time, the boundary condition of the stress in the plastic zone is

$$\begin{cases} \sigma_r\big|_{r=a} = p, \\ \sigma_r\big|_{r=r_p} = p_y. \end{cases} \tag{19}$$

Combining equations (18) and (19), we get

$$K = \left(p_y + \frac{\sigma_0}{M-1}\right) r_p^{(1-1/M)} = \left(p + \frac{\sigma_0}{M-1}\right) a^{(1-1/M)}. \tag{20}$$

Therefore, the stress solution in the plastic zone is

$$\begin{cases} \sigma_r = \left(p_y + \dfrac{\sigma_0}{M-1}\right)\left(\dfrac{r_p}{r}\right)^{M-1/M} - \dfrac{\sigma_0}{M-1}, \\ \sigma_\varphi = \dfrac{1}{M}\left(p_y + \dfrac{\sigma_0}{M-1}\right)\left(\dfrac{r_p}{r}\right)^{M-1/M} - \dfrac{\sigma_0}{M-1}. \end{cases} \tag{21}$$

Substituting the above equation (21) into the physical equation (5), the elastic strain solution in the plastic zone is obtained as

$$\begin{cases} \varepsilon_r^e = \dfrac{1}{2G}\left(1 - \nu - \dfrac{\nu}{M}\right)\left(p_y + \dfrac{\sigma_0}{M-1}\right)\left(\dfrac{r_p}{r}\right)^{M-1/M} - \dfrac{1-2\nu}{2G}\dfrac{\sigma_0}{M-1}, \\ \varepsilon_\varphi^e = \dfrac{1}{2G}\left(\dfrac{1-\nu}{M} - \nu\right)\left(p_y + \dfrac{\sigma_0}{M-1}\right)\left(\dfrac{r_p}{r}\right)^{M-1/M} - \dfrac{1-2\nu}{2G}\dfrac{\sigma_0}{M-1}, \end{cases} \tag{22}$$

where ε_r^e and ε_φ^e are radial elastic strain and tangential elastic strain in plastic zone, respectively.

From the basic assumption 3, combining equations (1) and (6), the strain increment in the plastic zone satisfies

$$\begin{cases} d_{\varepsilon_r^p} = d_\lambda \dfrac{\partial f}{\partial \sigma_r} = d_\lambda, \\ d_{\varepsilon_\varphi^p} = d_\lambda \dfrac{\partial f}{\partial \sigma_\varphi} = -M d_\lambda. \end{cases} \tag{23}$$

From the boundary condition of zero isotropic plastic strain at initial yielding, the plastic radial strain can be obtained by simultaneous the above equation (23)

$$\varepsilon_r^p = -\frac{1}{M}\varepsilon_\varphi^p. \tag{24}$$

The total radial and circumferential strain in the plastic zone include elastic strain and plastic strain

$$\begin{cases} \varepsilon_r = \varepsilon_r^e + \varepsilon_r^p, \\ \varepsilon_\varphi = \varepsilon_\varphi^e + \varepsilon_\varphi^p. \end{cases} \tag{25}$$

Combining equations (24) and (25) and substituting into the strain coordination equation (7), a first-order differential equation with r as the independent variable and ε_φ^p as the dependent variable is obtained

$$\frac{d\varepsilon_\varphi^p}{dr} + \left(1 + \frac{1}{M}\right)\frac{\varepsilon_\varphi^p}{r} + \frac{\varepsilon_\varphi^e - \varepsilon_r^e}{r} + \frac{d\varepsilon_\varphi^e}{dr} = 0. \tag{26}$$

Its general solution is

$$\varepsilon_\varphi^p = Cr^{-M+1/M} + \frac{1-\nu}{4G}\left(M - \frac{1}{M}\right)\left(p_y + \frac{\sigma_0}{M-1}\right)\left(\frac{r_p}{r}\right)^{M-1/M}. \tag{27}$$

From the boundary condition that the plastic strain at the boundary of the plastic zone is zero, the integral constant of the above formula can be solved as

$$C = -\frac{1-\nu}{4G}\left(M - \frac{1}{M}\right)\left(p_y + \frac{\sigma_0}{M-1}\right){r_p}^{M+1/M}. \tag{28}$$

Therefore, the plastic strain solution of the plastic zone is

$$\begin{cases} \varepsilon_r^p = \frac{1-\nu}{4GM}\left(M - \frac{1}{M}\right)\left(p_y + \frac{\sigma_0}{M-1}\right)\left(\frac{r_p}{r}\right)^{M+1/M} - \frac{1-\nu}{4GM}\left(M - \frac{1}{M}\right)\left(p_y + \frac{\sigma_0}{M-1}\right)\left(\frac{r_p}{r}\right)^{M-1/M}, \\ \varepsilon_\varphi^p = -\frac{1-\nu}{4G}\left(M - \frac{1}{M}\right)\left(p_y + \frac{\sigma_0}{M-1}\right)\left(\frac{r_p}{r}\right)^{M+1/M} + \frac{1-\nu}{4G}\left(M - \frac{1}{M}\right)\left(p_y + \frac{\sigma_0}{M-1}\right)\left(\frac{r_p}{r}\right)^{M-1/M}. \end{cases} \tag{29}$$

Furtherly, combining (22) and (29), the total plastic strain in the reign of $a < r < r_p$ can be obtained after finishing

$$\begin{cases} \varepsilon_r = \frac{1-\nu}{4GM}\left(M - \frac{1}{M}\right)\left(p_y + \frac{\sigma_0}{M-1}\right)\left(\frac{r_p}{r}\right)^{M+1/M} + \frac{2\nu-1}{2G}\frac{\sigma_0}{M-1} + \frac{1}{4GM}\left(M - M\nu - 2\nu + \frac{1}{M} - \frac{\nu}{M}\right)\left(p_y + \frac{\sigma_0}{M-1}\right)\left(\frac{r_p}{r}\right)^{M-1/M}, \\ \varepsilon_\varphi = -\frac{1-\nu}{4G}\left(M - \frac{1}{M}\right)\left(p_y + \frac{\sigma_0}{M-1}\right)\left(\frac{r_p}{r}\right)^{M+1/M} + \frac{2\nu-1}{2G}\frac{\sigma_0}{M-1} + \frac{1}{4G}\left(M - M\nu - 2\nu + \frac{1}{M} - \frac{\nu}{M}\right)\left(p_y + \frac{\sigma_0}{M-1}\right)\left(\frac{r_p}{r}\right)^{M-1/M}. \end{cases} \tag{30}$$

As the initial stress has been acting on the initial expansion radius in the initial state of slurry grouting expansion and the initial stress also produces the corresponding initial strain, there occurs a relative strain. And the relative strain value is the difference between the corresponding total plastic strain and the initial strain. According to the basic assumption 1 that the initial stress is isotropic which are all taken as p_0, the strain generated by the initial stress can be obtained from the physical equation (5) and expressed as

$$\varepsilon_r' = \varepsilon_\varphi' = \frac{1-2\nu}{2G}p_0. \tag{31}$$

Subtracting the corresponding radial and tangential strain values in equation (30) from equation (31), the relative strain solution in the plastic zone is

$$\begin{cases} \varepsilon_r = \frac{1-\nu}{4GM}\left(M - \frac{1}{M}\right)\left(p_y + \frac{\sigma_0}{M-1}\right)\left(\frac{r_p}{r}\right)^{M+1/M} + \frac{2\nu-1}{2G}\left(\frac{\sigma_0}{M-1} + p_0\right) + \frac{1}{4GM}\left(M - M\nu - 2\nu + \frac{1}{M} - \frac{\nu}{M}\right)\left(p_y + \frac{\sigma_0}{M-1}\right)\left(\frac{r_p}{r}\right)^{M-1/M}, \\ \varepsilon_\varphi = -\frac{1-\nu}{4G}\left(M - \frac{1}{M}\right)\left(p_y + \frac{\sigma_0}{M-1}\right)\left(\frac{r_p}{r}\right)^{M+1/M} + \frac{2\nu-1}{2G}\left(\frac{\sigma_0}{M-1} + p_0\right) + \frac{1}{4G}\left(M - M\nu - 2\nu + \frac{1}{M} - \frac{\nu}{M}\right)\left(p_y + \frac{\sigma_0}{M-1}\right)\left(\frac{r_p}{r}\right)^{M-1/M}. \end{cases} \tag{32}$$

Furtherly, by substituting the second term of the above equation into the geometric equation (4), the relative displacement of the plastic zone is

$$u_r = -\varepsilon_\varphi r = \frac{1-\nu}{4G}\left(M - \frac{1}{M}\right)\left(p_y + \frac{\sigma_0}{M-1}\right)\left(\frac{r_p}{r}\right)^{M+1/M} r - \frac{2\nu - 1}{2G}\left(\frac{\sigma_0}{M-1} + p_0\right) r - \frac{1}{4G}\left(M - M\nu - 2\nu + \frac{1}{M} - \frac{\nu}{M}\right)\left(p_y + \frac{\sigma_0}{M-1}\right)\left(\frac{r_p}{r}\right)^{M-1/M} r. \quad (33)$$

3.2. Design of Minimum Grouting Pressure. Since the minimum grouting pressure is the limit value to ensure the critical stable state of surrounding soils, there is a static balance between the radial expansion tension caused by grouting and the radial loose earth pressure caused by jacking excavation. As the value of grouting pressure is small, the corresponding expansion pressure is also small, the surrounding soil is considered to be in the elastic state ,and its radial stress solution can be solved according to the elastic solution of slurry grouting expansion.

As the soil around pipelines is deformed, extruded under the action of the reaming pressure and produces elastic radial displacement, the radial displacement value can indirectly reflect the change of the thickness of the mud sleeve. Therefore, assuming that the change in the thickness of mud sleeve is only affected by the slurry expansion pressure, the thickness of mud sleeve is the elastic relative radial displacement, which is shown in Figure 4. Its value can be expressed as

$$\delta = \frac{p - p_0}{2G} a. \quad (34)$$

Taking $r = a + \delta$ and substituting it into the first term of the elastic radial stress solution (10), the analytical solution of the radial expansion tension caused by grouting σ_δ can be obtained as

$$\sigma_\delta = p_0 + (p - p_0)\left(\frac{1}{1 + (p - p_0/2G)}\right)^2. \quad (35)$$

On the other hand, the excavation and jacking cause the loosening or collapse of the soil above and around the pipelines, so that the surrounding soil acts as loose earth pressure σ_n caused by jacking and excavation. What is more, in addition to acts in the vertical direction, the loose earth pressure also acts in the horizontal direction, so there occurs radial loose stress, and its value is the superposition of the vertical loose stress and the horizontal loose stress, as shown in Figure 5. Therefore, the radial loosening stress at any angle can be expressed as

$$\sigma_n = \sigma_V \sin\theta + \sigma_h \cos\theta, \quad (36)$$

where σ_V and σ_h are the vertical loose stress and the horizontal loose stress, respectively.

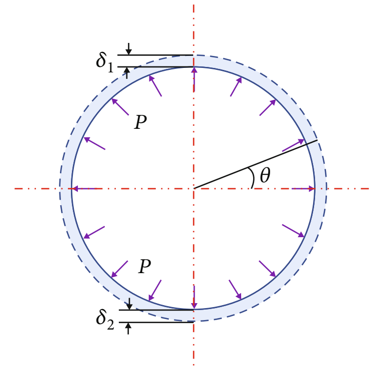

Figure 4: Schematic diagram of excavation hole deformation under expansion pressure.

The vertical loose stress and the horizontal loose stress can be expressed, respectively, as

$$\sigma_V = \sigma_{V1} + \gamma R_P - \gamma R_P \sin\theta, \quad (37)$$

$$\sigma_h = K_a(\sigma_{V1} + \gamma R_P - \gamma R_P \sin\theta), \quad (38)$$

where K_a is the active earth pressure coefficient, θ is the angle on a circular pipeline, σ_{V1} is the loose stress at the top of pipelines, and its value is generally solved by Terzaghi loose earth pressure theory and expresses as

$$\sigma_{V1} = k\gamma h, \quad (39)$$

where h is the burial depth at the top of pipelines, and k is the coefficient of Terzaghi earth pressure theory

$$k = \frac{1 - e^{-2K(\tan\delta)h/b}}{2K(\tan\delta)(h/b)}. \quad (40)$$

Combining equations (36), (37), (38), (39), and (40), we get the radial loose earth pressure caused by jacking excavation

$$\sigma_n = \left(k\gamma h + \gamma R_p - \gamma R_p \sin\theta\right)\left(\sin\theta + K_a \cos\theta\right). \quad (41)$$

By the condition of critical state of surrounding soil stability

$$\sigma_\delta = \sigma_n. \quad (42)$$

Combining equations (35) and (41), the minimum value of the expansion pressure $p_{u,\min}$ in the critical condition of the surrounding soil stability should satisfy

$$p_0 + \left(p_{u,\min} - p_0\right)\left(\frac{1}{1 + \left(p_{u,\min} - p_0/2G\right)}\right)^2 = \left(k\gamma h + \gamma R_p - \gamma R_p \sin\theta\right)\left(\sin\theta + K_a \cos\theta\right). \quad (43)$$

If the influence of hydrostatic pressure is considered, the

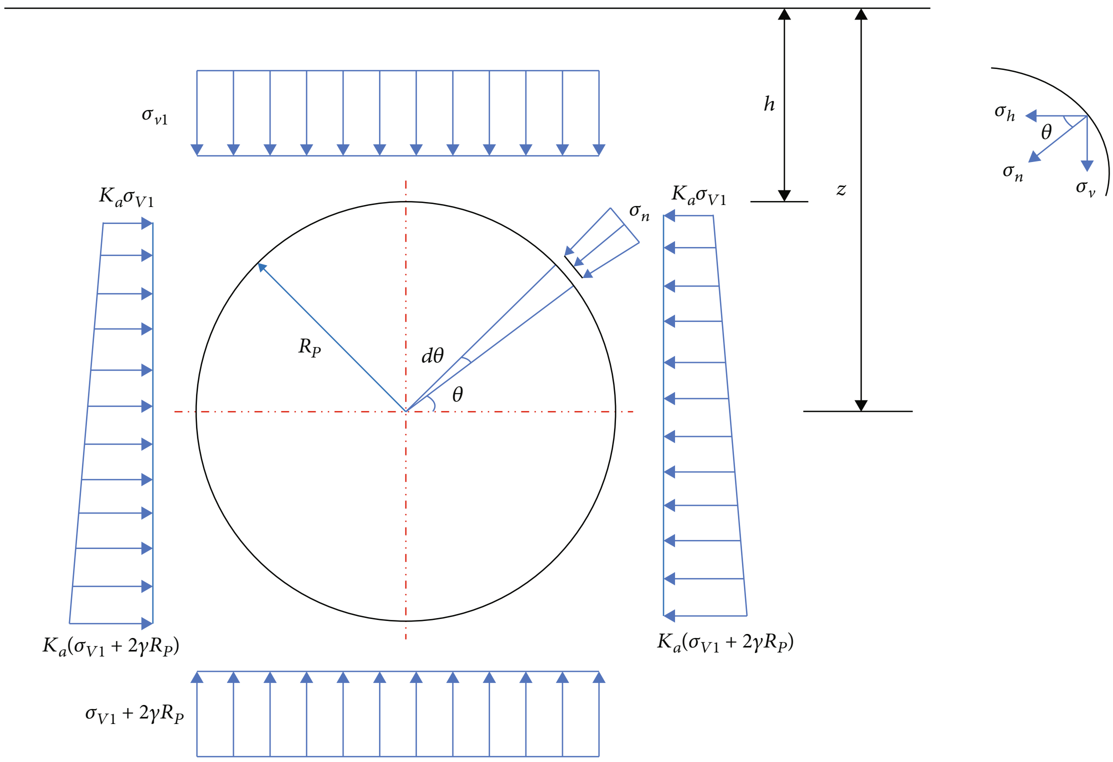

FIGURE 5: Distribution diagram of loose earth pressure.

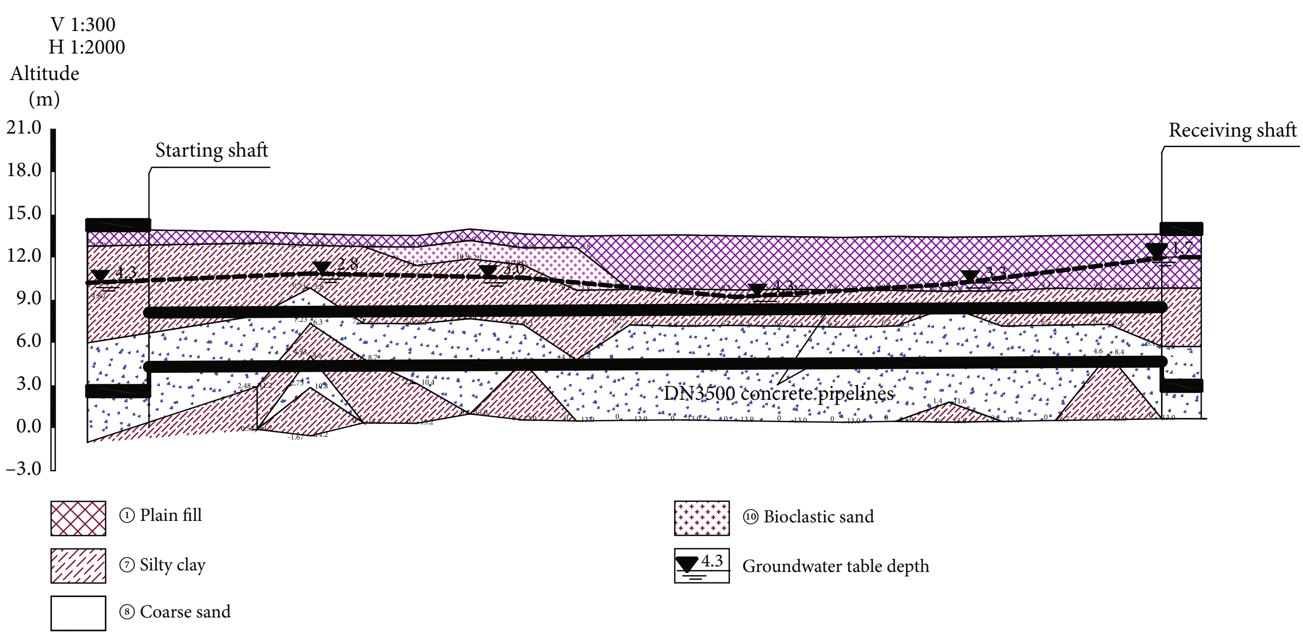

FIGURE 6: Geologic profile of the pipe jacking engineering.

minimum grouting pressure design value is

$$p_{s,\min} = p_{u,\min} + p_w. \tag{44}$$

But if the influence of groundwater in the soil is not considered, the hydrostatic pressure value can be considered to be zero.

3.3. Design of Maximum Grouting Pressure. When the grouting pressure increases to a certain degree, the slurry grouting expansion may change from grouting compaction to grouting splitting and have a splitting effect on the surrounding soil. Once the soil splits, the slurry will expand infinitely into the stratum, causing plastic deformation and land subsidence, and affecting the surrounding environment and the

Table 1: Main geotechnical parameters of soils at the construction site.

Soil layer	Depths (m)	Density (g/cm^3)	Water content (%)	Void ratio	Cohesion (kPa)	Internal friction angle (°)
(1) Plain fill	0-3.98	1.76	30.4	0.865	27.9	16.8
(2) Silty clay	3.98-6.58	1.84	25.03	0.81	14.91	15.42
(3) Coarse sand	6.58-13.28	2.65			8	30

Figure 7: Continued.

(e)

Figure 7: Site view of slurry grouting system and pipe jacking. (a) The head of pipe jacking machine. (b) Circulation slurry discharge in head. (c) Slurry synchronous grouting on segment. (d) Prefabricated grouting hole on each segment and the branch grouting pipe. (e) Ball valve controller.

stability of surrounding soils on the excavation face. Therefore, the maximum grouting pressure can be designed as the expansion pressure under the critical state of grouting splitting.

Due to the large deformation happens during grouting splitting, its analytical solution can be solved by the plastic solution of slurry grouting expansion. The displacement at the expanding hole is equal to the difference between the initial radius and the expanding radius which can be expresses as

$$\begin{aligned} a-a_0=u_r|_{r=a}=&\frac{1-\nu}{4G}\left(M-\frac{1}{M}\right)\left(p_y+\frac{\sigma_0}{M-1}\right)\left(\frac{r_p}{a}\right)^{M+1/M}a\\ &-\frac{2\nu-1}{2G}\left(p_0+\frac{\sigma_0}{M-1}\right)a\\ &-\frac{1}{4G}\left(M-M\nu-2\nu+\frac{1}{M}-\frac{\nu}{M}\right)\left(p_y+\frac{\sigma_0}{M-1}\right)\left(\frac{r_p}{a}\right)^{M-1/M}. \end{aligned} \tag{45}$$

Alternating equation (20), we get the ratio of critical plastic radius to expansion radius

$$\frac{r_p}{a}=\left(\frac{p+(\sigma_0/M-1)}{p_y+(\sigma_0/M-1)}\right)^{M/M-1}. \tag{46}$$

Combining (45) and (46), we can obtain

$$\begin{aligned} \frac{1}{\xi}=\frac{a_0}{a}=1&-\frac{1-\nu}{4G}\left(M-\frac{1}{M}\right)\left(p_y+\frac{\sigma_0}{M-1}\right)\left(\frac{p+(\sigma_0/M-1)}{p_y+(\sigma_0/M-1)}\right)^{M+1/M-1}\\ &+\frac{2\nu-1}{2G}\left(p_0+\frac{\sigma_0}{M-1}\right)\\ &+\frac{1}{4G}\left(M-M\nu-2\nu+\frac{1}{M}-\frac{\nu}{M}\right)\left(p+\frac{\sigma_0}{M-1}\right), \end{aligned} \tag{47}$$

where ξ is the rate of slurry expansion.

When the soil splits, the slurry expands infinitely, and the rate of slurry expansion ξ tends to infinity; then, the above equation (47) would tend to zero. Therefore, when the maximum expansion pressure $p_{u,\max}$ happens, it should satisfy

$$\begin{aligned} 1&-\frac{1-\nu}{4G}\left(M-\frac{1}{M}\right)\left(p_y+\frac{\sigma_0}{M-1}\right)\left(\frac{p_{u,\max}+(\sigma_0/M-1)}{p_y+(\sigma_0/M-1)}\right)^{M+1/M-1}\\ &+\frac{2\nu-1}{2G}\left(p_0+\frac{\sigma_0}{M-1}\right)\\ &+\frac{1}{4G}\left(M-M\nu-2\nu+\frac{1}{M}-\frac{\nu}{M}\right)\left(p_{u,\max}+\frac{\sigma_0}{M-1}\right)=0. \end{aligned} \tag{48}$$

This results in a maximum grouting pressure and expressed as

$$p_{s,\max}=p_{u,\max}+p_w. \tag{49}$$

Similar to the case of designing the minimum grouting pressure, when designing the maximum grouting pressure for waterless strata, the hydrostatic pressure value of the above formula can also be taken directly to zero.

4. Engineering and Verification

4.1. Engineering Background. This pipe jacking engineering is located near Meilan Airport in Meilan District, Haikou City. Its main task is to discharge the rainy season precipitation and municipal sewage around the airport and surrounding areas. The strata where the pipeline passes mainly composed of miscellaneous fill, silty clay, coarse sand, silty clay, and other soft soil. The environmental water in this project is mainly of groundwater in the exploration

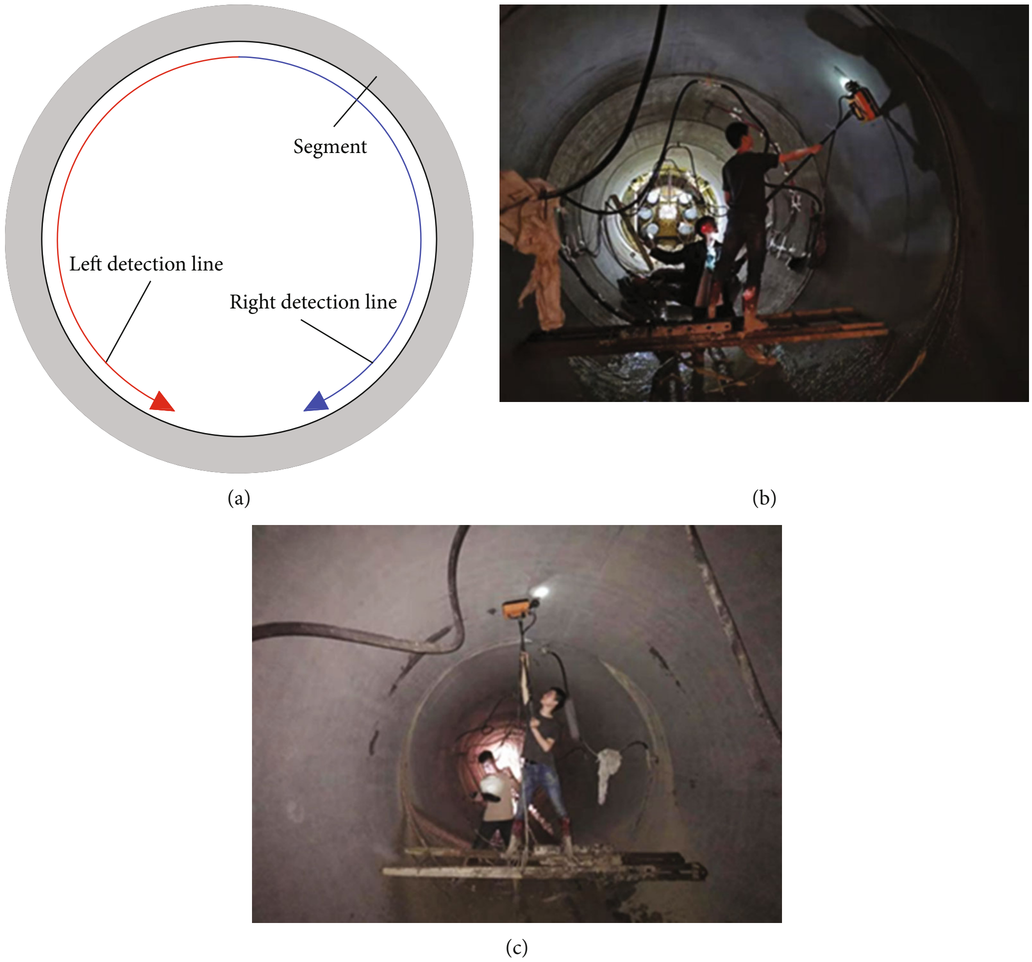

FIGURE 8: Geological radar detection design and data acquisition. (a) Design drawing of detection circuit. (b) Acquisition the right line. (c) Acquisition the left line.

borehole and surface water along the line. The buried depth of groundwater level is 1.90~4.10 m, and the average overburden depth is 5.85 m. The engineering geological profile and the corresponding geological parameters are shown in Figure 6 and Table 1.

The pipeline adopts circular prefabricated reinforced concrete segments with a width of 0.32 m. The inner diameter of the segment is 3.5 m, and the length is 2.5 m. To effectively bore through the soft soil layer, the MTBM is used in this project, whose whole length is 5.71 m, and the outer shell diameter is 4.16 m, as shown in Figure 7(a). Due to the soft stratum where this project is located, the slurry grouting system of synchronous grouting is adopted.

4.2. Design and Application. According to the geological conditions of this project, the strength criterion coefficients can be determined by formulas (2) and (3), in which the values are $M = 0.68$ and $\sigma_0 = 33.3$kPa, and the hydrostatic pressure is $p_w = 49.2$kPa. Based on the elastic-plastic theoretical solution of slurry grouting expansion deduced in this paper, the initial in situ stress of slurry grouting expansion is $p_0 = 209.88$kPa, and the critical plastic pressure is $p_y = 189.72$kPa. From formula (41), the values of radial loose soil stress are different at different angles. It can be determined as 24.8 kPa when it locates at the top of the pipe, takes as 134.6 kPa when it lies at the bottom of the pipe, takes as 26.3 kPa when it locates on the left and right side of the pipe. However, since the objective of this paper is to find the minimum grouting pressure, the radial loose soil stress at the top of the pipe is taken for solution. Considering the influence of hydrostatic pressure, the minimum grouting pressure is determined to be 0.15 MPa by equation (44), and the maximum grouting pressure of the project is determined to be 0.5 MPa by equation (49), and the design value of grouting pressure of this project is finally determined to be 0.3 MPa.

To ensure the smooth jacking of this project, the grouting system is reasonably arranged. After optimizing design according to the soil layer on site, the slurry is selected with the ratio of bentonite: soda ash: CMC: water = 15 : 6 : 0.2 : 78.8. The slurry is pumped by the ground hydraulic grouting pump through two pipelines, the inlet pipe and the discharge pipe, which is shown in Figure 7(b) and delivers to the tunnel boring machine's head and complete the slurry discharge cycle. At the same time, another pipeline system injects slurry into the prefabricated grouting holes of the segment and the gap at the end of the shield machine to

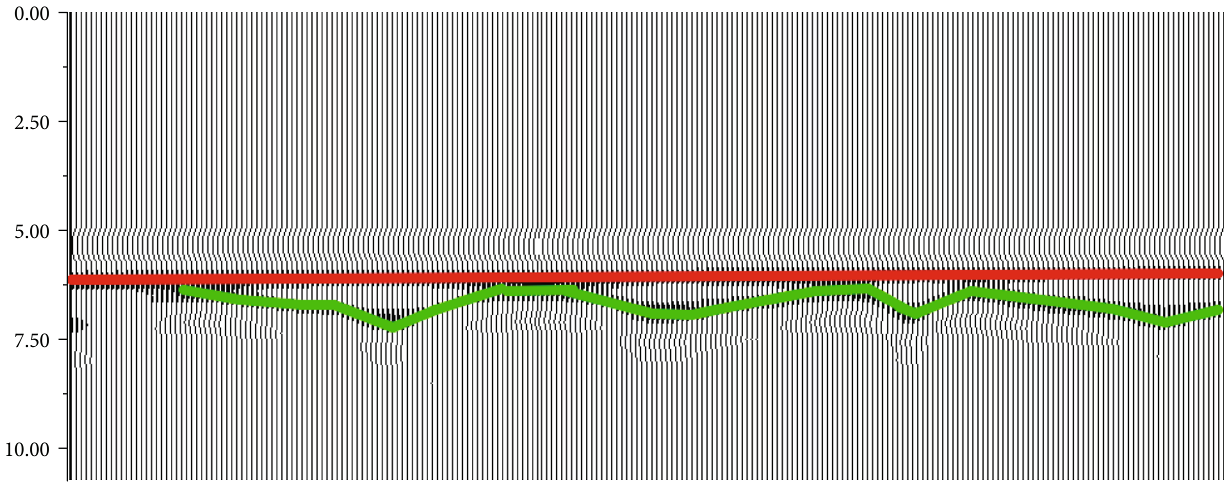

(a)

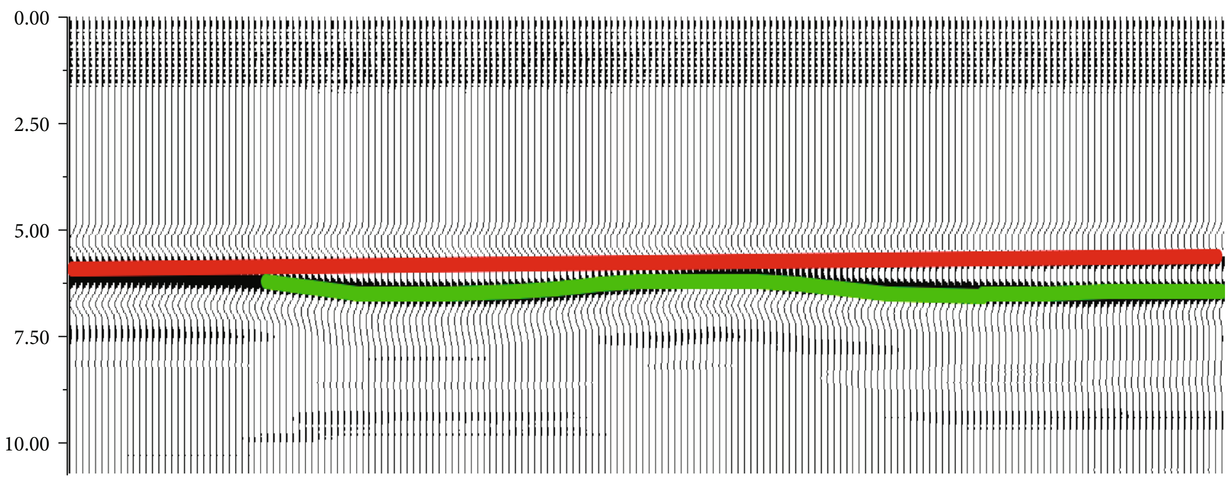

(b)

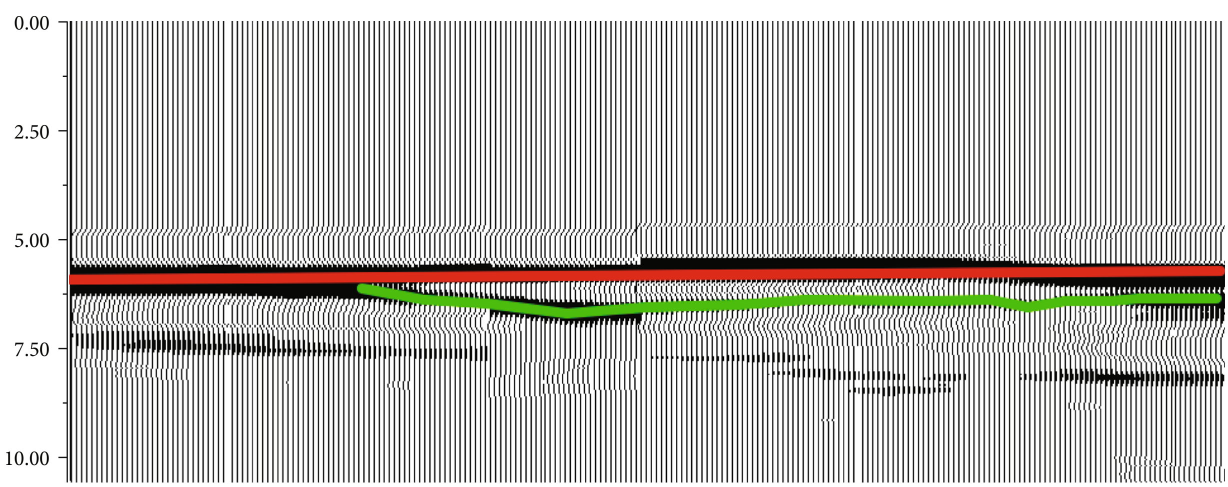

(c)

Figure 9: Continued.

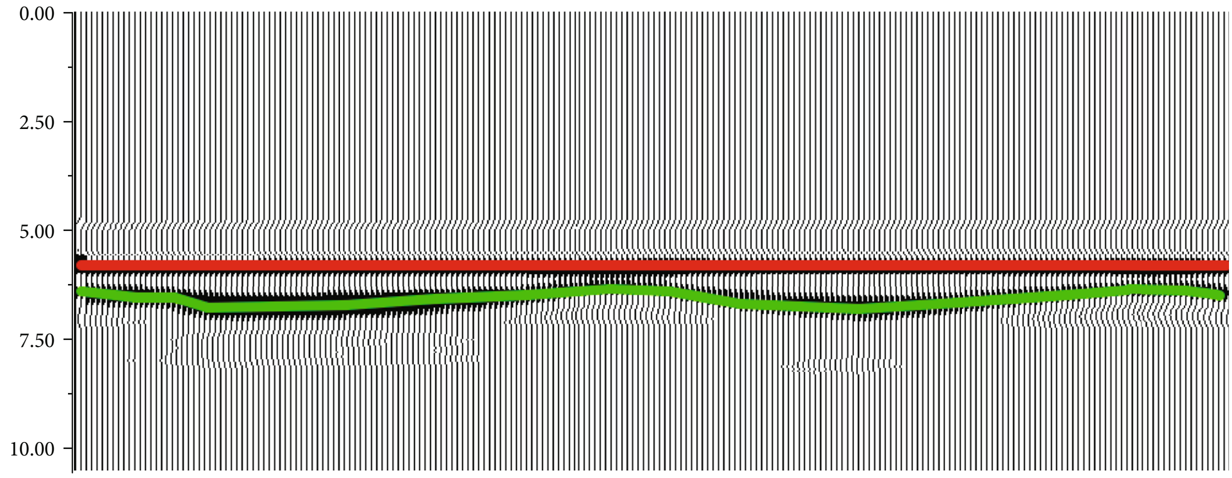

(d)

Figure 9: Geological radar map of segment detection. (a) Left side of the fourth pipe. (b) Right side of the fourth pipe. (c) Left side of the fifth pipe. (d) Right side of the fifth pipe.

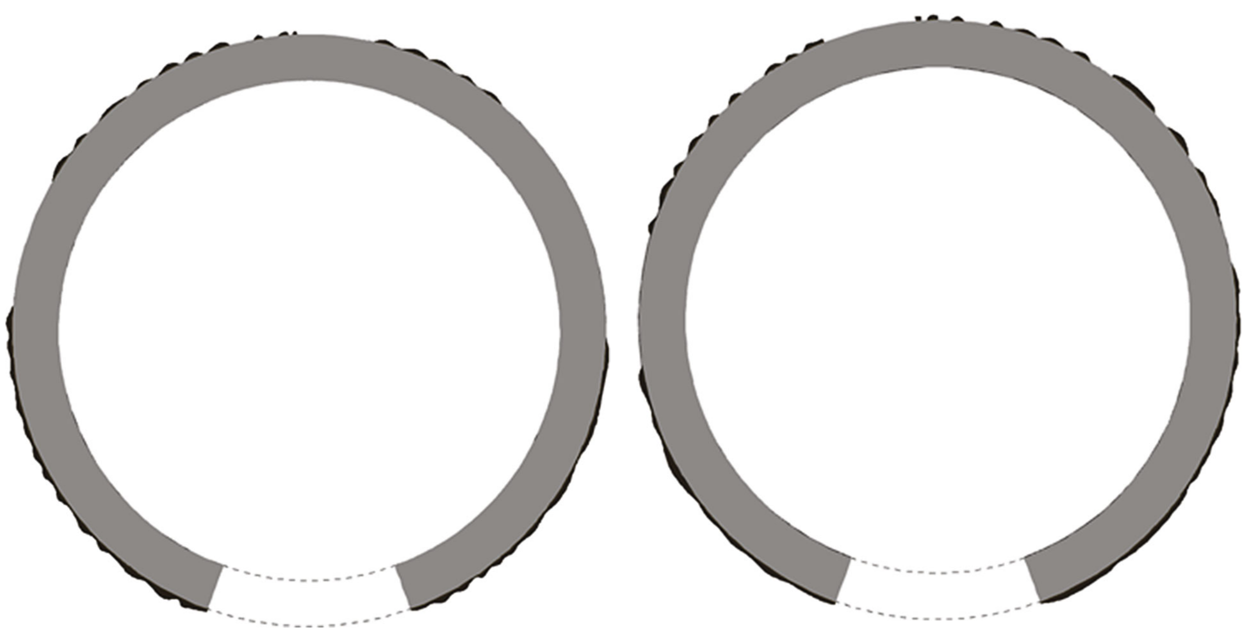

(a) (b)

Figure 10: Prediction diagram of slurry grouting distribution. (a) The fourth segment. (b) The fifth segment.

complete the slurry synchronous grouting of pipelines, as shown in Figure 7(c). Four grouting holes are reserved on each segment, which are, respectively, arranged in the upper, lower, left, and right directions of pipeline, as shown in Figure 7(d). Each grouting hole is separately controlled by DN25 ball valve, and the grouting hole is connected with DN25 rubber pipe and connected to the main grouting pipe, as shown in Figure 7(e). DN50 galvanized steel pipe is used for the main grouting pipe and DN25 pressure resistant rubber pipe is used for the branch pipe, and a stainless steel diaphragm pressure gauge is set every 100 m to control the grouting pressure. Synchronous grouting shall be carried out along with jacking during construction, and each segment shall be carried out in sequence according to jacking sequence. Grouting shall be carried out firstly and then jacking in follow. The whole grouting process is controlled and supervised by stainless steel pressure gauge. The whole slurry grouting system during pipe jacking is shown in Figure 7.

4.3. Field Test and Engineering Verification. In order to evaluate the design effectiveness and the rationality of the grouting system in depth, field tests were conducted by using geological radar detection technology. Due to the different dielectric constant and electromagnetic wave absorption effect between different media, different reflected waves will

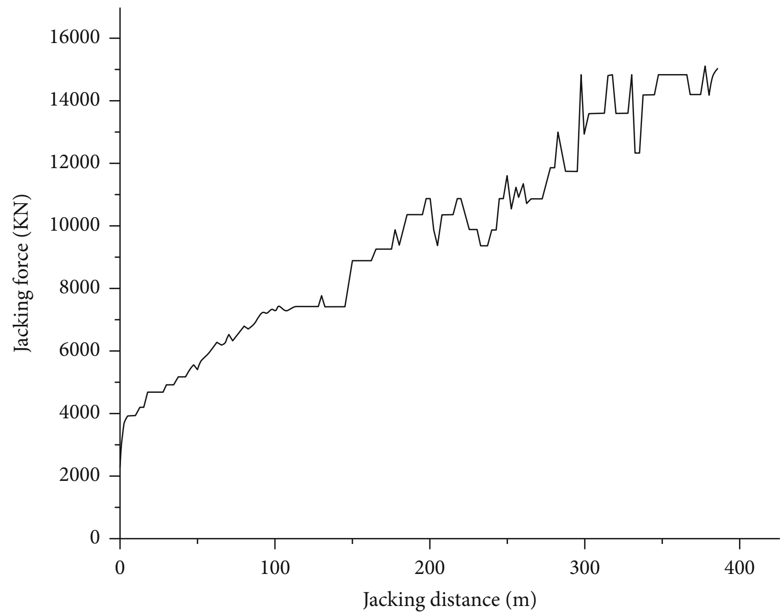

Figure 11: Measured jacking force and friction resistance on site.

be formed at the media partition interface, the distribution of reflected waves reflects the relative position of segment and slurry, and the distribution of slurry grouting layer thickness as well. Therefore, the conclusions measured and analyzed by GPR detection technology can verify whether the grouting pressure value designed by theory is reasonable and meets the engineering needs to a certain extent.

In this pipe jacking engineering, when the jacking distance reached 35 m, the on-site geological radar exploration was carried out for the 4th and 5th segment of pipelines, respectively. Since there were equipment wires and the inlet pipe and the discharge pipe at the bottom of the pipeline which needed to avoid during actual detection, the detection line was designed to divide into left and right sides along the inner wall of the segment, respectively. The LTD series ground-penetrating radar of China Institute of Radio Wave Propagation was used to monitor and collect data, and the basic setting parameters of this geo-radar were antenna frequency 900 GHz, sampling point 121, time window 25 ns, and antenna movement step 0.01 m. The detection route and field acquisition are shown in Figure 8.

The analysis of data is processed by the software provided by the instrument, and the preprocessing works such as direct wave removal, channel average, point average, automatic unsmooth gain adjustment, low-pass filtering, and background noise elimination are completed separately. Then, the monitoring results of the left and right sides of the 4th and 5th segment can obtain, as shown in Figure 9.

In Figure 9, there are two obvious strong reflected waves, in which the reflected wave of the red line reflects the concrete segment and the green curve reflects the slurry outside the segment. The red line is evenly distributed along the detection line, and the green line acts on the outer wall of the segment and is continuous distributed along the detection line basically, but the thickness distribution of the slurry is not uniform. As the time difference of the take-off point between the first strong reflection wave and the second strong reflection wave is about 0.7 ns to 2 ns, adopting the recommended values in reference [37] that the propagation speed of electromagnetic wave between slurry is about 0.03~0.055 m/ns, the thickness of filter cake can be furtherly determined that is about 10 mm to 55 mm, and the prediction diagram of filter cake distribution can be obtained, which is shown in Figure 10.

At the same time, the jacking force during the pipe jacking was also recorded on site, as shown in Figure 11. It can be seen that the friction resistance in the whole process is basically stable at about 32.9 kPa, and the increase of jacking force is steady without obvious sudden increase or sudden drop. The effect of slurry grouting on resistance reduction is stable and obvious.

From the above field tests and observations, it can be seen that the grouting system designed in this project can effectively support the stratum and protect the surrounding environment. There is no soil collapse around pipelines due to the instability of surrounding soil, and the soil near excavation hole is statically balanced and stable. What is more, the effect of friction resistance reduction is stable and significant. Therefore, the design of slurry grouting pressure in this project is reasonable, and the on-site construction scheme is scientific and effective.

5. Conclusions

Aiming at the background that the theoretical research of grouting pressure is far from the development of engineering needs, this paper raises a new theoretical calculation method, and its applicability and rationality are proved by a practical slurry pipe jacking engineering, which solves the actual engineering demand to a certain extent.

(1) Based on the influence characteristics of slurry on pipe-soil contact force and surrounding environment, this paper puts forward that reasonable grouting pressure should ensure good frictional resistance reduction effect and effective protection of surrounding environment. The core of these two design objectives is to ensure the stability of surrounding soil, and the design value of grouting pressure can be deduced from the corresponding necessary conditions

(2) With the injection of slurry, the interaction between soil-slurry-pipe is inevitable. The interaction between pipe-soil-slurry during synchronous grouting and the influence of grouting pressure on the stability of surrounding soil are analyzed. The mechanical model of slurry grouting expansion on surrounding soils is established, and the corresponding elastic and elastoplastic analytical solutions are deduced, which lays a theoretical foundation for designing grouting pressure

(3) As the jacking excavation and grouting disturbance occur at the same time during synchronous grouting, the radial expanding stress caused by grouting disturbance and the loose earth pressure caused by excavation jacking all act on the excavation hole and determine the stability of surrounding soils in common. Therefore, the minimum grouting pressure can be obtained from the static balance between them. And the maximum grouting pressure can be designed from the critical grouting splitting pressure

(4) Due to the endless engineering problems, the theoretical study of grouting is still far from the engineering demand of technology. The theoretical solution of grouting pressure raised in this paper is only applicable to the general engineering of grouting in slurry pipe jacking, without considering the influence of slurry properties, components, and adaptability of special stratum, etc., which needs to be improved in the future

Data Availability

All data generated or analyzed during this study are included in this article.

Conflicts of Interest

The authors declare that there are no conflicts of interest regarding the publication of this article.

Acknowledgments

The authors acknowledge the financial support provided by the National Natural Science Foundation of China (nos. 51874005 and 51778004) and the Science Research Foundation for Young and Middle-aged Academic Backbones in Anhui University of Science and Technology.

References

[1] R. L. Sterling, "Developments and research directions in pipe jacking and microtunneling," *Underground Space*, vol. 5, no. 1, pp. 1–19, 2020.

[2] Y. Ye, L. Peng, W. Yang, Y. Zou, and C. Cao, "Calculation of friction force for slurry pipe jacking considering soil-slurry-pipe interaction," *Advances in Civil Engineering*, vol. 2020, Article ID 6594306, 10 pages, 2020.

[3] X. Yang, Y. Liu, and C. Yang, "Research on the slurry for long-distance large-diameter pipe jacking in expansive soil," vol. 2018, Article ID 9040471, Advances in Civil Engineering, 2018.

[4] K. Wen, W. Zeng, H. Shimada, T. Sasaoka, and A. Hamanaka, "Numerical and theoretical study on the jacking force prediction of slurry pipe jacking traversing frozen ground," *Tunnelling and Underground Space Technology*, vol. 115, article 104076, 2021.

[5] GB-50268-2008, *Code for Construction and Acceptance of Water and Sewerage Pipeline Words*, The Ministry of Construction of China & General Administration of Quality Supervision, Inspection and Quarantine of the People's Republic of China, Beijing, China, 2008.

[6] Japan Microtunnelling Association, *Microtunnelling Methods Serious II, Design, Construction Management and Rudiments*, Japan Microtuuuenling Assocaition, Tokyo, Japan, 2013.

[7] Z. Zhong, C. Li, X. Liu, Y. Xiong, Y. Fan, and N. Liang, "Assessment of experimental friction parameters and contact property of pipe string for the estimation and verification of a solution for pipe stuck in the China's first rock pipe jacking," *Tunnelling and Underground Space Technology*, vol. 107, article 103671, 2021.

[8] K. Shou, J. Yen, and M. Liu, "On the frictional property of lubricants and its impact on jacking force and soil-pipe interaction of pipe-jacking," *Tunnelling and Underground Space Technology*, vol. 25, no. 4, pp. 469–477, 2010.

[9] B. Tang, Z. Wang, H. Cheng et al., "Experimental study on pipe strength and field performance of pipe jacking TBM in deep-buried coal mines," *International Journal of Civil Engineering*, vol. 19, no. 11, pp. 1327–1338, 2021.

[10] B. Tang, H. Cheng, Y.-Z. Tang et al., "Experiences of gripper TBM application in shaft coal mine: a case study in Zhangji coal mine, China," *Tunnelling and Underground Space Technology*, vol. 81, pp. 660–668, 2018.

[11] B. Tang, H. Cheng, Y. Tang et al., "Supporting design optimization of tunnel boring machines-excavated coal mine roadways: a case study in Zhangji, China," *Processes*, vol. 8, no. 1, p. 46, 2020.

[12] Z. Niu, Y. Cheng, Y. Zhang, Z. Song, G. Yang, and H. Li, "A new method for predicting ground settlement induced by pipe jacking construction," *Mathematical Problems in Engineering*, vol. 2020, Article ID 1681347, 11 pages, 2020.

[13] C. Wang, J. Liu, H. Cheng, and H. Cai, "Disturbance effect of pipe jacking group adjacent excavation on surrounding soil," vol. 2021, Article ID 5533952, Advances in Civil Engineering, 2021.

[14] D.-J. Ren, Y.-S. Xu, J. Shen, A. Zhou, and A. Arulrajah, "Prediction of ground deformation during pipe-jacking considering multiple factors," *Applied Sciences*, vol. 7, pp. 1051–1060, 2018.

[15] W. Ke and J. Lai, "Analysis of grouting impact on soil displacement in pipe jacking construction," in *International Conference on Pipelines and Trenchless*, pp. 463–472, Xi'an, China, 2014.

[16] G. Wei, R. Q. Xu, J. M. Shao, M. L. Luo, and Z. L. Jin, "Research on mechanism of reducing firction through injecting slurry in pipe jacking," *Rock and Soil Mechanics*, vol. 25, pp. 930–934, 2004.

[17] H. Shimada, T. Sasaoka, S. Khazaei, Y. Yoshida, and K. Matsui, "Performance of mortar and chemical grout injection into surrounding soil when slurry pipe-jacking method is used," *Geotechnical & Geological Engineering*, vol. 24, no. 1, pp. 57–77, 2006.

[18] M. Namli and E. Guler, "Effect of bentonite slurry pressure on interface friction of pipe jacking," *Journal of Pipeline Systems Engineering and Practice*, vol. 8, no. 2, article 04016016, 2017.

[19] K. Staheli, *Jacking Force Prediction: An Interface Friction Approach Based on Pipe Surface Roughness, School of Civil and Environmental Engineering, [Ph.D. thesis]*, Georgia Institute of Technology, Atlanta, GA, USA, 2006.

[20] W. C. Cheng, G. Li, and D. E. Ong, "Lubrication performance of pipejacking in soft alluvial deposits," *Tunnelling and Underground Space Technology*, vol. 91, article 102991, 2019.

[21] W. Long, B. Fu, P. Ji, and C. X. Chang, "Study on clay-free slurry used for Long-distance pipeline jacking," *Exploration Engineering*, vol. 39, pp. 68–70, 2012.

[22] L. C. Wang, Y. Q. Zhao, W. Long, Y. L. Guo, and Z. Q. Zhu, "Research on the wall protection slurry system of large diameter pipe jacking across deep desert and its application," *Geology and Exploration*, vol. 56, pp. 163–172, 2020.

[23] C. T. Wang and W. Long, "Experimental study on the slurry formulation used for the large diameter long distance pipe jacking project," *Journal of Reilweu Science and Engineering*, vol. 11, pp. 106–111, 2014.

[24] W. Cui, D. Liu, H. F. Song, and G. J. Pu, "Development and experimental study on environmental slurry for slurry shield tunneling," *Construction and Building Materials*, vol. 2016, pp. 416–423, 2019.

[25] B. Yuan, Z. Li, Z. Zhao, H. Ni, Z. Su, and Z. Li, "Experimental study of displacement field of layered soils surrounding laterally loaded pile based on transparent soil," *Journal of Soils and Sediments*, vol. 4, pp. 1–12, 2021.

[26] B. Yuan, M. Sun, Y. Wang, L. Zhai, Q. Luo, and X. Zhang, "Full 3D displacement measuring system for 3D displacement field of soil around a laterally loaded pile in transparent soil," *International Journal of Geomechanics*, vol. 19, no. 5, article 04019028, 2019.

[27] B. Yuan, Z. Li, W. Chen et al., "Influence of groundwater depth on pile–soil mechanical properties and fractal characteristics under cyclic loading," *Fractal and Fractional*, vol. 6, no. 4, p. 198, 2022.

[28] B. Yuan, M. Chen, W. Chen et al., "Effect of pile-soil relative stiffness on deformation characteristics of the laterally loaded pile," *Advances in Materials Science and Engineering*, vol. 2022, Article ID 4913887, 13 pages, 2022.

[29] F. Ye, H. W. Gou, Z. J. Duan, X. Liang, S. Y. Wang, and B. Wang, "Disturbance mechanical problems induced by synchronous grouting in deep shield tunnels," *Chinese Journal of Rock Mechanics and Engineering*, vol. 41, pp. 855–863, 2019.

[30] F. Ye, C. F. Guo, J. H. Mao, P. B. Yang, Z. Chen, and T. Jia, "Calculation of critical grouting pressure during shield tunneling in clay stratum," *Rock and Soil Mechanics*, vol. 36, pp. 937–945, 2015.

[31] J. F. Zou, L. Li, X. L. Yang, and Z. N. Hu, "Mechanism analysis of fracture grouting in soil," *Rock and Soil Mechanics*, vol. 27, pp. 626–628, 2006.

[32] J. F. Zou, W. G. Xu, Q. Luo, L. Li, and X. L. Yang, "Study on grouting pressure of fracture grouting in saturated soil," *Rock and Soil Mechanics*, vol. 29, pp. 1802–1806, 2008.

[33] S. H. Jia, C. F. Zhao, and C. Zhao, "Analysis of expanded radius and internal expanding pressure of cylindrical hole," *Chinese Journal of Rock Mechanics and Engineering*, vol. 34, pp. 182–188, 2015.

[34] W. J. Han, S. Y. Liu, D. W. Zhang, and C. Y. Gu, "Numerical simulation of pressure-controlled cavity expansion," *Rock and Soil Mechanics*, vol. 31, pp. 405–411, 2010.

[35] Y. N. Li and W. Li, "Theoretical analysis of expanded radius and internal expanding pressure of the spherical (cylindrical) cavity expansion," *Chinese Journal of Applied Mechanics*, vol. 37, pp. 142–148, 2020.

[36] S. K. A. Au, A. T. Yeung, and K. Soga, "Pressure-controlled cavity expansion in clay," *Canadian Geotechnical Journal*, vol. 43, pp. 714–725, 2006.

[37] J. Du, H. W. Huang, and X. Y. Xie, "Application of dielectric permittibity of grouting materical to GPR image identification," *Rock and Soil Mechanics*, vol. 27, pp. 1219–1223, 2006.